Journal of Clinical Imaging Science

Editor-in-Chief: Vikram S. Dogra, MD
Department of Imaging Sciences, University of Rochester Medical Center, Rochester, USA

OPEN ACCESS
HTML format

For entire Editorial Board visit : www.clinicalimagingscience.org/editorialboard.asp

www.clinicalimagingscience.org

REVIEW ARTICLE

Establishing a Chest MRI Practice and its Clinical Applications: Our Insight and Protocols

Christine U. Lee, Darin B. White, Anne-Marie G. Sykes

Department of Radiology, Mayo Clinic, Rochester MN, USA

Address for correspondence:
Dr. Christine Lee,
Department of Radiology, Mayo Clinic,
200 Frist Street SW, Rochester MN
55905, USA.
E-mail: lee.christine@mayo.edu

Received : 20-12-2013
Accepted : 28-02-2014
Published : 21-03-2014

ABSTRACT

Despite its nonionizing technique and exquisite soft tissue characterization, noncardiovascular, and nonmusculoskeletal magnetic resonance imaging (MRI) of the chest has been considered impractical due to various challenges such as respiratory motion, cardiac motion, vascular pulsatility, air susceptibility, and paucity of signal in the lung. With advances in MRI, it is now possible to perform diagnostically useful and good quality MRIs of the chest, but literature on subspecialized chest MRI practices is limited. The purpose of this manuscript is to describe the rationale, nuances, and logistics that went into developing such a practice in the Division of Thoracic Radiology at our institution. The topics addressed include technical and clinical considerations, support at administrative and clinical levels, protocol development, and economic considerations compared with conventional practices. Various MRI techniques are also specifically discussed to facilitate chest MRI at other sites. Although chest MRI is used in a relatively small number of patients at this point, in certain patients, chest MRI can provide additional information to optimize medical management. A few clinical cases illustrate the quality and clinical utility of chest MRI. Given recent advances in MRI techniques, it is now an opportune time to develop a chest MRI practice.

Key words: Chest magnetic resonance imaging, protocols, practice, thoracic MRI

INTRODUCTION

"Order an MRI of the chest? Can we do that?"
"I am not aware of any clinical indications for lung MR at this time."
"Medical training mantra (albeit more than 10 years ago) was to never order an MRI of the chest."
"How much does a chest MRI cost compared to a CT?"

These were some comments from many of our clinical and even radiology colleagues when our Division of Thoracic Radiology broached the idea of developing a subspecialty chest magnetic resonance imaging (MRI) practice over a year ago. We believed that MRI could provide soft tissue characterization and insights into noncardiovascular and nonmusculoskeletal chest pathology not otherwise attainable with traditional imaging of the chest such as radiographs, computed tomography (CT), and positron

Access this article online	
Quick Response Code:	Website: www.clinicalimagingscience.org
	DOI: 10.4103/2156-7514.129288

This article may be cited as:
Lee CU, White DB, Sykes AG. Establishing a Chest MRI Practice and its Clinical Applications: Our Insight and Protocols. J Clin Imaging Sci 2014;4:17.
Available FREE in open access from: http://www.clinicalimagingscience.org/text.asp?2014/4/1/17/129288

Table 1: Chest MRI scanning parameters on a siemens 1.5T magnet

Series no.	Series description	Resp. tech.	Siemens							
			Pulse sequence	FOV (cm)	Matrix size (ph × freq)	Slice thick. (mm)	TR/TE (ms/ms)	No. of slices	BW (Hz/Px)	Other parameters
1	Scout	FB	HASTE	44	192 × 256	8	900/84	8 sag; 5 cor; 15 ax	407	-
2	Coronal T2	BH	BLADE TSE	36	256 × 256	5	3000/171	30	501	BLADE coverage = 120% Turbo factor = 71 IPAT = 2 Concatenations = 5
3	Coronal 2D bSSFP	FB	TRUE FISP	42	256 × 256	4 with −60% gap	415/1.16	128	1028	Single shot
4	Navigator scout	FB	HASTE	44	192 × 256	8	900/84	15 cor; 9 ax	407	-
5	Axial T2	NT	BLADE TSE	36	320 × 320	5.5	var/96	41	300	Turbo factor = 30 BLADE coverage = 200%
6	Axial DWI	RT	EPSE	38	160 × 160	5.5	var/81	41	2084	Averages = 4 IPAT = 2
7	Pregadolinium T1 3D SPGR	BH	Dixon VIBE with CAIPARINHA	34	162 × 288	3.3	6.09/2.339/ (TE_2 4.78)	var	300/1020	Flip angle = 12 Acceleration = 4
8	Test Bolus	FB	FLASH GRE	40	197 × 256	18	35.08/1.43 (min TR/min TE)	1	400	-
9	Postgadolinium T1 3D SPGR	BH	Dixon VIBE with CAIPARINHA	34	162 × 288	3.3	6.09/2.339/ (TE_2 4.78)	var	300/1020	Flip angle = 12 Acceleration = 4
10 (opt)	T1 SPGR In-and out-of-phase	BH	(From series 7)							
11 (opt)	Axial bSSFP	BH	TRUE FISP	38	204 × 256	5 skip 1	(Parameter optimization still under investigation)			
12 (opt)	Cine bSSFP	FB	TRUE FISP	42	256 × 256	4	415/1.16	1	1028	Single shot

FOV: Field of view, TR: Repetition time, TE: Echo time, BW: Bandwidth, FB: Free-breathing, RT: Respiratory-triggered, NT: Navigator-triggered, ph: Phase, freq: Frequency, Px: Pixel, sag: Sagittal, cor: Coronal, ax: Axial, Thick: Thickness, Resp. Tech: Respiration technique, opt: Optional, Ph Accel: Phase acceleration, var: Variable, BH: Breath hold

Table 2: Chest MRI scanning parameters on a GE 1.5T magnet

Series no.	Series description	Resp. tech.	GE							
			Pulse sequence	FOV (cm)	Matrix size (freq × ph)	Slice thick. (mm)	TR/TE (ms/ ms)	No. of slices	BW (Hz)	Other parameters
1	Scout	FB	SSFSE	48	352 × 192	10		15 ax 7 sag 11 cor	62.50	-
2	Coronal T2	BH	FRFSE	40	256 × 256	6, skip 1	2250/102	32	50	ETL = 19
3	Coronal 2D bSSFP	FB	2D FIESTA	40	192 × 256	4, skip 2	3.5/min TE	118	100	-
4	Axial T2	RT	PROPELLER FSE	38	320	5, skip 1	var/101	20	125	ETL = 32 Nex = 3 Refocus angle = 160 PhAccel = 3
5	Axial DWI	RT	EPI	38	128 × 128	6, skip 1	min TE	27	83.33	-
6	Pregadolinium T1 3D SPGR	BH	LAVA-Flex with ARC	35	320 × 224	4	6.6/min TE	60	83.33	Flip angle = 12
7	Test bolus	FB	GRE	40	256 × 128	6	13.7/min TE	1	62.5	-
8	Postgadolinium T1 3D SPGR	BH	LAVA-Flex with ARC	35	320 × 224	4	6.6/min TE	60	83.33	Flip angle = 12
9 (opt)	T1 SPGR in-and out-of-phase	BH	SPGR	40	256 × 192	5, skip 1	140/2.1/ (TE_2 4.4)	var	62.5	Flip angle = 70
10 (opt)	Axial bSSFP	BH	2D FIESTA	40	192 × 256	5, skip 2	3.5/1.2	var	125	-
11 (opt)	Cine bSSFP	FB	2D FIESTA	40	192 × 224	5, skip 2	3.5/1.2	1	125	-

FOV: Field of view, TR: Repetition time, TE: Echo time, BW: Bandwidth, FB: Free-breathing, RT: Respiratory-triggered, NT: Navigator-triggered, ph: Phase, freq: Frequency, Px: Pixel, sag: Sagittal, cor: Coronal, ax: Axial, Thick: Thickness, Resp. Tech: Respiration technique, opt: Optional, Ph Accel: Phase acceleration, var: Variable, BH: Breath hold

Series 4: Navigator scout

The purpose of this series is to optimize placement of a 2D navigator for subsequent navigator-triggered acquisitions. Navigator Scout images are HASTE/SSFSE acquisitions, which, at first glance, may seem like a redundant series to the Scout Series. We have observed that: (1) initial anxiety can lead to erratic diaphragmatic motion, which is generally allayed this far into the examination, making tracking of the right hemi-diaphragm more regular at this point of the examination, and (2) we can obtain a more reliable location of the posterior aspect of the dome of the liver on an axial slice, which is an optimal place for navigator placement. Some patients who have had surgery on the right side may have suboptimal right hemi-diaphragmatic excursion, and in those instances, we have been successful in placing the navigator on the left hemi-diaphragm at the level of the spleen.

time can be particularly important for patients who are dyspneic, anxious, or who have trouble lying supine for a prolonged time, all fairly common occurrences in our patient population.

RADIOLOGY ECONOMICS

Regarding cost, the nominal fee of an MRI without and with contrast costs almost twice as much as a CT without and with contrast, and the Medicare fee (in the United States) for an MRI costs about 1.7 times as much as a comparable CT. In terms of relative value units (RVU, a metric in the United States designed to measure physicians' work activity in uniform units), the only comparison available is a nonspecified chest MRI with and without contrast that generates roughly 10 times the RVUs for a chest X-ray and about 1.6 times that for a chest CT. Higher reimbursement for MRI is probably related to a number of factors, including initial cost of the equipment, maintenance, and patient throughput; however, the examination time for an individual patient does not affect the cost of the examination, since the length of the time slots are predetermined. We do believe that examinations should be as short as possible, particularly in a patient population that may have limited tolerance for long breath-holds or even lying supine for an extended period.

CASES

In many cases, the exquisite soft tissue detail from MRI provides great benefit in guiding clinical decision-making and patient management [Figures 1-5].

Case 1

A 32-year-old male with biopsy-proven sarcomatoid carcinoma involving the right middle lobe was evaluated by MRI. Figure 1 shows an example of the right middle lobe malignant mass suspicious of pericardial invasion, a finding confirmed at surgery. In this case, T2-weighted images using a BLADE TSE/PROPELLER FSE technique and ECG-gated double inversion-recovery FSE images were particularly useful in characterizing disease extent.

Case 2

A 25-year-old female with chromosomal abnormality, and severe combined pectus excavatum and carinatum deformity presented with a large mediastinal mass. T2-weighted and contrast-enhanced T1-weighted images illustrate the exquisite soft tissue contrast, detail, and extent of a complicated cystic mass consistent with lymphatic malformation [Figure 2].

Case 3

A 45-year-old female with chronic upper respiratory symptoms and dry cough had an MRI as part of her imaging work-up. Contrasting soft tissue signaling features in the mediastinum can be particularly improved with some MRI techniques such as DWI [Figure 3] as shown in this case. Based on the imaging features differential considerations included thymoma and left phrenic nerve sheath tumor. Surgery followed with pathology indicating a thymoma with extensive cystic change.

Case 4

A 53-year-old male with a large left hemithorax mass could not tolerate lying supine in the MRI scanner, and the entire study was performed with the patient in the left lateral

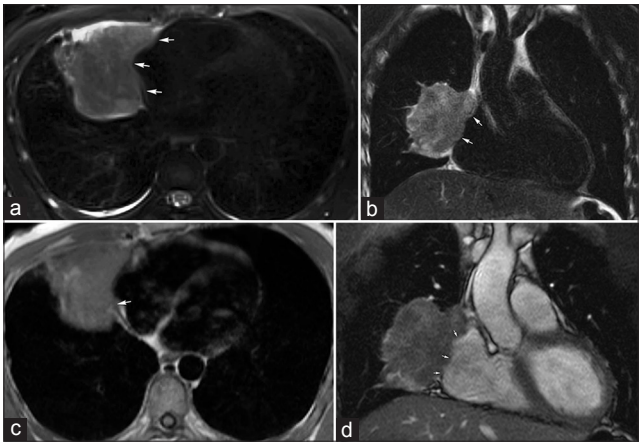

Figure 1: 32-year-old male with biopsy-proven sarcomatoid carcinoma involving the right middle lobe. MRI was performed to evaluate disease extent. (a) Axial and (b) coronal T2-weighted images using a PROPELLER/BLADE technique demonstrate the lobulated right middle lobe mass invading the mediastinal fat medially (arrows). (c) Gated double inversion-recovery FSE "black-blood" image shows the loss of the hypotense pericardial line (arrow), and (d) real-time free-breathing bSSFP image shows lack of apparent separation (arrows) highly suspicious for pericardial invasion, a finding confirmed at surgery.

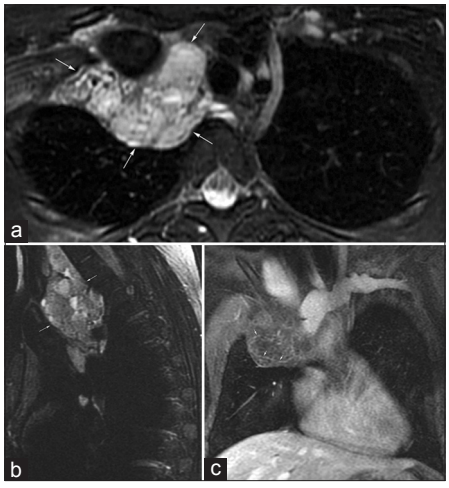

Figure 2: 25-year-old female with chromosomal abnormality, mediastinal mass, and severe combined pectus excavatum and carinatum deformity. (a) Axial and (b) sagittal T2-weighted images demonstrate a multilobulated, multiseptated cystic mass (arrows) with multiple fluid-fluid levels in the right side of the superior mediastinum extending into the right side of the neck and to the junction of the superior vena cava and the right atrium. (c) Coronal postcontrast T1-weighted image demonstrates thin septal enhancement (arrows). Findings are consistent with a large lymphatic malformation for which the patient had previously undergone surgery.

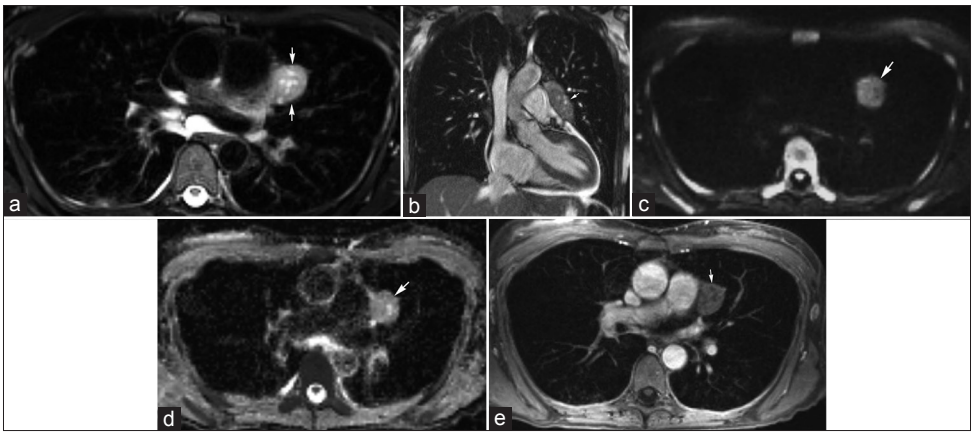

Figure 3: A 45-year-old female with chronic upper respiratory symptoms and dry cough. (a) Axial T2-weighted image and (b) coronal bSSFP image demonstrate an elongated rounded mass (arrows) with internal cystic areas along the course of the left phrenic nerve. (c) Diffusion-weighted image using b=800 s/mm^2 and correlating (d) apparent diffusion coefficient (ADC) map show no appreciable restricted diffusion (arrow). (e) Contrast-enhanced axial image demonstrates minimal enhancement of this mass (arrow). Differential considerations include thymoma and left phrenic nerve sheath tumor. The mass was resected with pathology indicating a thymoma with extensive cystic change.

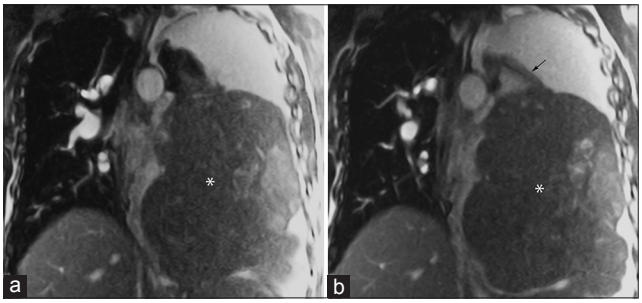

Figure 4: 53-year-old male with a large left hemithorax mass. (a and b) Coronal noncontrast-enhanced real-time free-breathing bSSFP images demonstrate a large extra-pulmonary mass (*) that arises from the left inferior pulmonary ligament (arrow). Differential considerations include sarcoma or fibrous tumor of the pleura. This was surgically excised with pathology indicating solitary fibrous tumor with focal tumoral necrosis.

decubitus position. For patients who cannot lie supine or who are severely short of breath, noncontrast-enhanced fast imaging techniques such as bSSFP can provide helpful information [Figure 4]. Differential considerations included sarcoma or fibrous tumor of the pleura. The mass was surgically excised with pathology indicating solitary fibrous tumor with focal tumoral necrosis.

Case 5

An 85-year-old male with malignant mesothelioma presented with focal right-sided anterior pain. Staging of mesothelioma by CT and PET/CT may benefit from improved soft tissue contrast provided by MRI particularly along the mediastinal pleura [Figure 5]. The region of focal pain corresponded to a mass, which demonstrated restricted diffusion.

CONCLUSION

Noncardiovascular nonmusculoskeletal chest MRI is at the optimal time for implementation, and several topics

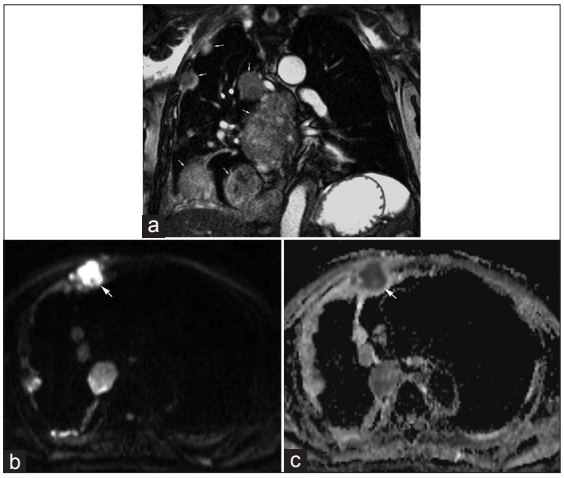

Figure 5: 85-year-old male with malignant mesothelioma having focal right-sided anterior pain. (a) Coronal real-time free-breathing bSSFP image illustrates multiple pleural masses (arrows) consistent with known malignant mesothelioma. (b) Diffusion-weighted image using b=800 s/mm^2 and corresponding (c) apparent diffusion coefficient (ADC) map demonstrate restricted diffusion in one of the pleural masses (arrow). The location of this mass corresponded with the region of focal pain.

discussed here help to provide practical steps and insight to developing a thriving chest MRI practice. With appropriate teams and protocols in place, the complications of chest MRI imaging can be overcome to provide the diagnostic imaging quality of soft tissue detail that can make a difference in clinical decision making and patient management.

ACKNOWLEDGMENTS

The authors would like to acknowledge Peter D. Kollasch, who joined them with both feet running and has never slowed down. Without his time, expertise, and dedication, the authors would not be where they are now. The authors also acknowledge the assistance of Sonia Watson, Ph.D., with manuscript preparation.

REFERENCES

1. Biederer J, Beer M, Hirsch W, Wild J, Fabel M, Puderbach M, et al. MRI of the lung (2/3). Why ... when ... how? Insights Imaging 2012;3:355-71.
2. Biederer J, Hintze C, Fabel M, Jakob P, Horger W, Graessner J, et al. MRI of the Lung – ready … get set … go! Magnetom Flash 2011;1:6-14.
3. Biederer J, Mirsadraee S, Beer M, Molinari F, Hintze C, Bauman G, et al. MRI of the lung (3/3)-current applications and future perspectives. Insights Imaging 2012;3:373-86.
4. Biederer J, Puderbach M, Hintze C. A Practical Approach to Lung MRI at 1.5T. Magnetom Flash 2006;238-43.
5. Puderbach M, Hintze C, Ley S, Eichinger M, Kauczor HU, Biederer J. MR imaging of the chest: A practical approach at 1.5T. Eur J Radiol 2007;64:345-55.
6. Wielputz M, Kauczor HU. MRI of the lung: State of the art. Diagn Interv Radiol 2012;18:344-53.
7. Wild JM, Marshall H, Bock M, Schad LR, Jakob PM, Puderbach M, et al. MRI of the lung (1/3): Methods. Insights Imaging 2012;3:345-53.
8. Lane BF, Vandermeer FQ, Oz RC, Irwin EW, McMillan AB, Wong-You-Cheong JJ. Comparison of sagittal T2-weighted BLADE and fast spin-echo MRI of the female pelvis for motion artifact and lesion detection. AJR Am J Roentgenol 2011;197:W307-13.
9. Plathow C, Schoebinger M, Herth F, Tuengerthal S, Meinzer HP, Kauczor HU. Estimation of pulmonary motion in healthy subjects and patients with intrathoracic tumors using 3D-dynamic MRI: Initial results. Korean J Radiol 2009;10:559-67.
10. Takahashi K, Inaoka T, Murakami N, Hirota H, Iwata K, Nagasawa K, et al. Characterization of the normal and hyperplastic thymus on chemical-shift MR imaging. AJR Am J Roentgenol 2003;180:1265-9.

Source of Support: Nil, **Conflict of Interest:** None declared.